Proceedings of CHT-15
ICHMT International Symposium on Advances in Computational Heat Transfer

May 25-29, 2015, Rutgers University, Piscataway, USA

CHT-15-083

DEPENDENCE OF NUMERICAL SMEARING AND RAY EFFECT IN DISCRETE-ORDINATES METHOD

Brian Hunter and Zhixiong Guo[§]
Dept. of Mechanical and Aerospace Engineering, Rutgers University, Piscataway, NJ, USA
[§]Correspondence author. Email: guo@jove.rutgers.edu

ABSTRACT

Solutions of the integro-differential equation of radiation transfer via numerical methods were well known to suffer from two distinct shortcomings: (1) numerical smearing error due to spatial domain discretization, and (2) ray effect error due to angular discretization. In this study, it is shown that both error types exhibit dependence on both spatial and angular discretization. Proportionality expressions for various orders of numerical smearing errors are derived, and ray effect is categorized into local and propagation errors. Using the DOM, it is found that refinement of spatial grid can reduce both error types without a necessary change in direction number, while increase in direction number mandates a necessary increase in spatial refinement to minimize error sources.

INTRODUCTION

Numerical methods have become increasingly demanded in the field of radiation heat transfer, as many applications require accurate solutions to the Equation of Radiation Transfer (ERT) [Modest 2002, Howell et al. 2011]. In the presence of radiation scattering, the ERT is an integro-differential equation, and analytic solutions are nearly impossible in multi-dimensional geometries. Thus, to accurately determine radiation heat transfer contributions, various numerical methods have been developed. Solution of the ERT using numerical methods involves the discretization of both the spatial and angular domains, which result in two major types of numerical error: (1) false scattering and (2) ray effect, which were first discovered in the discrete-ordinates method (DOM) [Chai et al. 1993]. Actually, such types of errors exist in all ERT-discretization based methods including the finite-volume method (FVM).

"False scattering" was named because this type of error tends to mimic the behavior of scattering by artificially smoothening the intensity field. It is a direct result of spatial discretization practices, and is significant in multidimensional problems where spatial grid lines and radiation directions are misaligned, although it still persists in 1-D problems [Raithby 1997, Coelho 2002]. "False scattering" is also referred to as "numerical smearing" [Coelho 2002] and is dependent on both spatial grid resolution and chosen spatial differencing scheme. After the discovery of the third type of numerical error - angular false scattering [Hunter and Guo 2012] - it is appropriate to call the false scattering error as numerical smearing.

Ray effect stems from the approximation of the double integral in total solid angle 4π using a finite number of discrete radiation directions [Chai et al. 1993]. Lack of appropriate angular resolution can lead to physically unrealistic bumps and oscillations in the intensity field. Ray effect exists in any method where angular discretization exists, although the degree of error magnitude may differ for different solution methods and different directional quadrature schemes [Hunter and Guo 2013]. Ray

effect and numerical smearing have been shown to exhibit compensatory effects in some situations, such that reduction of one error may increase another error [Coelho 2002].

In this study, a detailed investigation into numerical smearing and ray effect after DOM discretization is presented. The dependence of numerical smearing and ray effect on both spatial and angular discretization is revealed. Proportionality expressions for various orders of numerical smearing are derived, and ray effect is characterized into local and propagation components. Comparisons of DOM heat fluxes with benchmark MC predictions are shown, in order to illustrate the appearance of each numerical error. Additionally, error impact is analysed for varying optical properties.

DISCRETIZATIONS OF ERT

In general vector notation, the steady-state ERT of radiation intensity I can be expressed as follows, for a gray, absorbing-emitting, and scattering medium [Menguc and Viskanta 1985, Modest 2002]:

$$\hat{\boldsymbol{s}} \cdot \nabla I(\boldsymbol{r}, \hat{\boldsymbol{s}}) = -(\sigma_a + \sigma_s) I(\boldsymbol{r}, \hat{\boldsymbol{s}}) + \sigma_a I_b(\boldsymbol{r}) + \frac{\sigma_s}{4\pi} \oiint_{4\pi} I(\boldsymbol{r}, \hat{\boldsymbol{s}}') \Phi(\hat{\boldsymbol{s}}', \hat{\boldsymbol{s}}) d\Omega' \tag{1}$$

where Eq. (1) represents a balance between spatial gradients of radiation intensity and intensity augmentation/attenuation due to absorption, emission, and scattering. Using the DOM, Eq. (1) can be expanded into a simultaneous set of partial differential equations in many discrete directions for a general 3-D enclosure, defined using Cartesian coordinates, in the following dimensionless form:

$$\mu^l \frac{\partial I^l}{\partial \tau_x} + \eta^l \frac{\partial I^l}{\partial \tau_y} + \xi^l \frac{\partial I^l}{\partial \tau_z} = -I^l + (1-\omega) I_b + \frac{\omega}{4\pi} \sum_{l'=1}^{M} w^{l'} \Phi^{l'l} I^{l'}, \qquad l = 1,2,\dots,M \tag{2}$$

where $\tau_j = (\sigma_a + \sigma_s) j$ for $j = x, y, z$, and the scattering albedo $\omega = \sigma_s/(\sigma_a + \sigma_s)$. The continuous angular integral of radiation scattering is replaced by a sum over M total discrete directions, defined by both polar angle θ^l and azimuthal angle ϕ^l. To solve Eq. (2) using an iterative CV marching procedure, the spatial domain of interest is discretized into numerous control-volumes (CVs), and the spatial derivatives are approximated using control-volume (CV) differencing methods. Additional details on the DOM and solution procedure can be found in textbooks [Modest 2002, Howell et al. 2011] and references [Menguc and Viskanta 1985, Hunter and Guo 2012].

NUMERICAL SMEARING

Numerical smearing error arises due to domain spatial discretization [Chai et al. 1993, Coelho 2002]. Consider the derivative $\mu^l \frac{\partial I^l}{\partial \tau_x}$, with domain discretized using the CV schematic in Figure 1, and three representative discretization schemes to approximate the derivative: the step scheme, diamond scheme, and QUICK scheme:

$$\mu^l \left(\frac{\partial I^l}{\partial \tau_x}\right)_i \cong \mu^l \left(\frac{I_i^l - I_{i-1}^l}{\Delta \tau_x}\right)_{step} \cong \mu^l \left(\frac{I_{i+1}^l - I_{i-1}^l}{2\Delta \tau_x}\right)_{diam} \cong \mu^l \left(\frac{3I_{i+1}^l + 3I_i^l - 7I_{i-1}^l + I_{i-2}^l}{8\Delta \tau_x}\right)_{QUICK} \tag{3}$$

where $\Delta \tau_x = (\sigma_a + \sigma_s)\Delta x$. Derivative approximation introduces numerical smearing in the form of truncation error, which can be readily determined using Taylor Series analysis. The highly-stable step scheme attains first order $O(\Delta \tau_x)$ accuracy with respect to grid size $\Delta \tau_x$, while the diamond and QUICK schemes are second-order accurate $O(\Delta \tau_x^2)$.

In general, Taylor Series analysis shows that the numerical smearing error inherent in an $O(\Delta \tau_x^n)$ spatial differencing scheme $\left|E_x^{l,n}\right| \propto \left|\mu^l \Delta \tau_x^n \frac{\partial^{n+1}(I^l)}{\partial \tau_x^{n+1}}\right|$. From the ERT, $\mu^l \frac{\partial I^l}{\partial \tau_x} \sim -I^l$, and thus $\frac{d^n(I^l)}{d\tau_x^n} \sim \left(-\frac{1}{\mu^l}\right)^n I^l$. Additionally, according to the Beer-Lambert Law, $I^l = I_0^l e^{-\frac{\Delta \tau_x}{\mu^l}}$. Using a 1st-order

Taylor series approximation for e^{-x}, $I^l \sim \left(1 - \frac{\Delta\tau_x}{\mu^l}\right)$, and thus $\frac{d^n(I^l)}{d\tau_x^n} \sim \left(-\frac{1}{\mu^l}\right)^n \left(1 - \frac{\Delta\tau_x}{\mu^l}\right)$. Finally, via substitution, the following proportionality relationship for numerical smearing error is derived:

$$\left|E_x^{l,n}\right| \propto \left|\left(\frac{\Delta\tau_x}{\mu^l}\right)^n \left(1 - \frac{\Delta\tau_x}{\mu^l}\right)\right| \tag{4}$$

From Eq. (4), it is apparent that numerical smearing error can be reduced by either refining spatial grid density, reducing medium optical thickness, or by using higher-order spatial schemes. To confine numerical smearing error, $\left(\frac{\Delta\tau_x}{\mu^l}\right)_{max}$ should not be greater than 1, as the function $|x^n(1-x)|$ rapidly diverges towards infinity for $x > 1$. Additionally, this condition becomes more critical as n increases.

Numerical smearing itself was widely believed to be "independent" of angular discretization. However, Eq. (4) illustrates that numerical smearing error depends directly on the ratio of spatial grid size to discrete direction cosine magnitude. Therefore, refinement of angular grid will actually increase numerical smearing error for constant grid size, due to reduction in μ^l. Moreover, the total numerical smearing error can be expressed using the root-sum-squares (RSS) method as follows, for 3-D problems:

$$E_{NS} = \sqrt{\sum_{l=1}^{M} \left[\left(E_x^{l,n}\right)^2 + \left(E_y^{l,n}\right)^2 + \left(E_z^{l,n}\right)^2\right]} \tag{5}$$

Eq. (5) reinforces the dependence of overall numerical smearing error on angular discretization, showing that increasing M (i.e., refining angular direction/reducing ray effect) will increase E_{NS}.

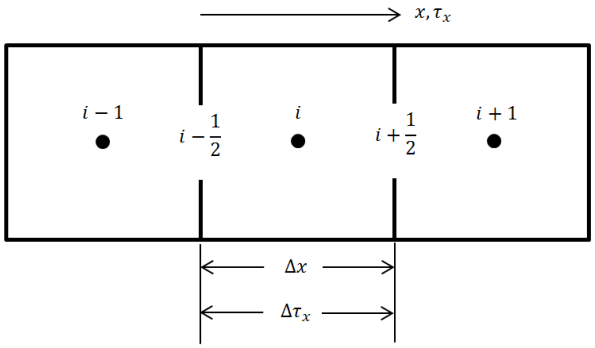

Figure 1: Typical 1-D spatial discretization

RAY EFFECT

Ray effect error results from the approximation of the continuous angular variation of radiation scattering via a finite number of discrete directions [Chai et al. 1993, Coelho 2002] and is comprised of two components: (1) local error and (2) propagation error. The local component arises from the difference between the exact scattering integral and the approximate summation for each discrete direction:

$$(RE)^l = \left[\oint\!\!\oint_{4\pi} I(\boldsymbol{r}, \hat{\boldsymbol{s}}')\Phi(\hat{\boldsymbol{s}}', \hat{\boldsymbol{s}})d\Omega' - \sum_{l'=1}^{M} \Phi^{l'l} I^{l'} w^{l'}\right] \tag{6}$$

Additionally, local ray effect error also exists in the determination of radiative quantities of interest, such as wall heat flux q_w incident radiation G, and divergence of radiative heat flux $(\nabla \cdot q)$:

$$(RE)_{q_w} = \left[\oint\!\!\oint_{4\pi} I(\boldsymbol{r}_w, \hat{s}')(\hat{s}' \cdot \boldsymbol{n}_w)d\Omega' - \sum_{l'=1}^{M} I^{l'} w^{l'} (\hat{s}^{l'} \cdot \boldsymbol{n}_w)\right] \tag{7a}$$

$$(RE)_G = \left[\oint\!\!\oint_{4\pi} I(\boldsymbol{r}_w, \hat{s}')d\Omega' - \sum_{l'=1}^{M} I^{l'} w^{l'} \right] = \frac{-(RE)_{\nabla \cdot q}}{\sigma_a} \tag{7b}$$

The propagation component of ray effect error arises from the propagation of rays. Consider the 2-D computational domain in Figure 2a, where a diffuse emitter is located at the bottom wall and the medium is purely absorbing. For simplicity, the diffuse radiation is approximated using two radiation directions (A & A'), represented by the dashed lines. Tracing rays in these two directions from the source wall illustrates the expansion of the radiation sphere with increasing propagation distance, resulting in no direct ray interception at CVs 1-4. Physically, all CVs should receive radiation from the diffuse emitter. This prevailing notion was broadly adopted to explain ray effect. As seen in Figure 2b, however, the propagating rays are actually incorporated into adjacent CV boundaries, and the radiation sphere effectively resets with new CVs of interest. Therefore, the arrows in Figure 2b represent a more appropriate view of ray propagation during DOM calculation. For example, ray 1 in CV-1 is affected by ray A, and ray 1' is affected by ray A'. Ray 3 in CV-3 is additionally impacted by ray A via ray 1, and so on. As a matter of fact, all CVs in the calculation domain do receive radiation from the emitter in practical DOM calculations. Due to the finite number of rays during propagation, errors arise. Increasing ray number M is the most effective way to reduce ray effect.

Ray effect error was widely thought to be independent of spatial discretization. This statement may not be true. Through refinement of the spatial grid (see Figure 2c), one can see that ray propagation error can be effectively reduced without increasing ray number. Additionally, according to the Beer-Lambert Law, in a given CV, intensity decays exponentially with $\Delta\tau$. Thus, by refining the spatial grid, the magnitude of ray attenuation in a given CV is significantly decreased, which could enhance local errors of ray effect. Therefore, the possibility exists that changes in spatial grid can have a significant impact on ray effect, although no practical method to separate these errors from grid-dependent numerical smearing errors is apparent.

Considering the relationship in Eq. (4), reduction of propagation ray effect via spatial grid refinement (reduction of $\Delta\tau_x$) can additionally reduce numerical smearing error. However, it should be emphasized again, increasing discrete direction number M under constant $\Delta\tau_x$ will reduce the minimum values of μ^l, dramatically increasing the corresponding E_x^l errors. Thus, an important conclusion is that while reduction of $\Delta\tau_x$ may not necessitate a corresponding change in μ^l, reduction in μ^l requires a corresponding reduction in $\Delta\tau_x$ so that both ray effect and numerical smearing errors are minimized. Such disclosure of these relationships with rigorous analyses is new to the field.

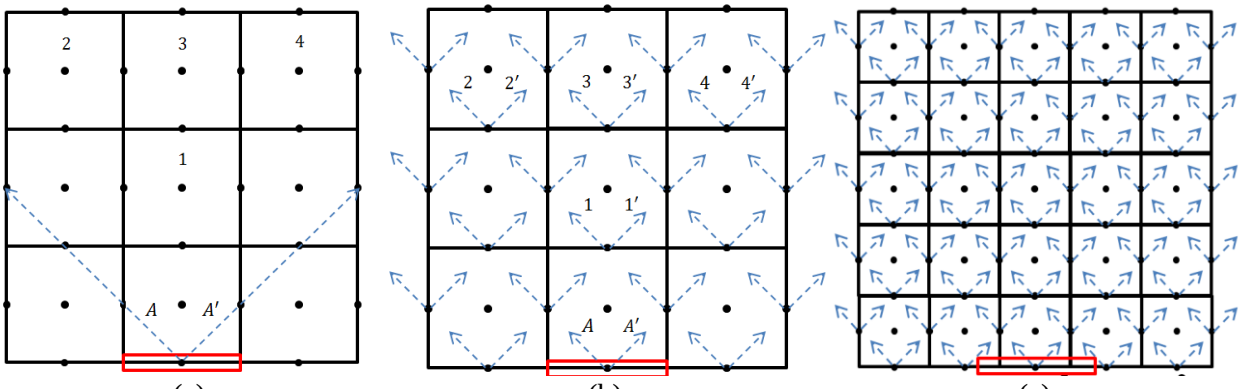

(a) (b) (c)

Figure 2: Illustration of propagation ray effect and possible reduction of propagation error via refinement of spatial grid

RESULTS AND DISCUSSION

To support the derivations and explanations in the previous section, an analysis of the impact of ray effect and numerical smearing errors on radiative transfer predictions using the DOM is presented. The benchmark test problem analysed involves steady-state radiation transfer in a cubic enclosure of edge length L, housing an absorbing-scattering medium, with optical thickness $\tau = (\sigma_a + \sigma_s)L$ and single scattering albedo ω. The medium is assumed to scatter light anisotropically according to the Henyey-Greenstein (HG) phase-function approximation [Modest 2002], and thus the asymmetry factor of the medium is taken as g. Non-dimensionalization of the spatial coordinates by the enclosure edge length is implemented, i.e.: $x^* = x/L$. The medium and enclosure walls are taken to be cold and black, except for the wall at $z^* = 0$, which is taken as a diffuse emitter with unity emissive power. Unless otherwise stated, the positive spatial differencing scheme, which guarantees positive intensities and can attain up to 2nd-order accuracy [Modest 2002, Coelho 2002], and the $SRAP_N$ geometric, equal-weight quadrature scheme are implemented.

An illustration of numerical smearing errors is presented in Figure 3, in which dimensionless heat fluxes generated at the centerline $(y^* = 0.5, z^* = 1.0)$ of the wall opposite the source wall in the benchmark problem are plotted for various spatial grid resolutions and optical properties. In order to solely gauge errors due to numerical smearing, $M = 160$ discrete directions are used, as a direction-independency test (not shown here, for conciseness) revealed that such direction number limits ray effect error. DOM heat fluxes are compared to benchmark Monte Carlo (MC) predictions [Boulet et al. 2007], generated with over 4 million quanta for each reference CV using $\Delta x^* = 0.05$. Figure 3 shows that errors due to numerical smearing are highly prevalent for lower spatial resolutions in the thicker medium (τ = 10.0). Improvement in spatial grid resolution improves conformity to MC predictions. For τ = 1.0, numerical smearing errors are minimal for all spatial grid resolutions, as $\Delta\tau_x \ll 1$ for most grids used.

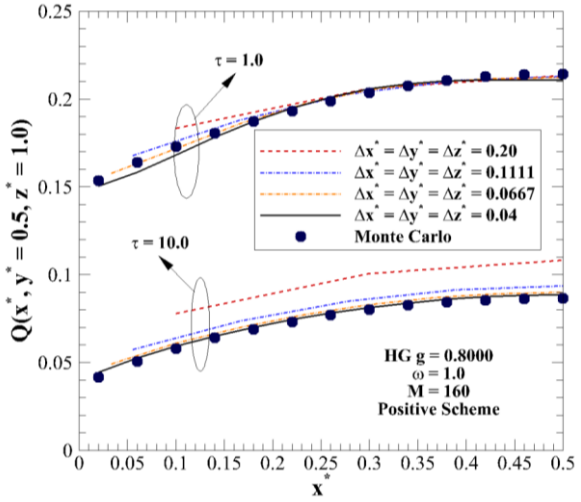

Figure 3: Illustration of numerical smearing due to spatial discretization (MC results from [Boulet et al. 2007]).

Figure 4a plots numerical smearing error in DOM heat flux at the center of the far wall, i.e. $Q(x^* = 0.5, y^* = 0.5, z^* = 1.0)$ versus $\Delta\tau$ for various optical thicknesses. The benchmark heat fluxes for comparison are generated using $\Delta\tau_x = 0.01$, 0.10, 0.20, and 0.20 for τ = 1.0, 5.0, 10.0, and 20.0, respectively. The results show that numerical smearing error decreases with spatial grid refinement. Additionally, for all optical thicknesses, the error curves effectively collapse to a single curve, indicating that numerical smearing errors depend directly on $\Delta\tau$, as deduced from the previous analysis of Eq. (4). Figure 4b plots numerical smearing error versus spatial grid size for various spatial differencing schemes in an isotropically scattering medium with τ = 5.0. For this analysis, the benchmark solution is generated using the 3rd-order SMART differencing scheme with $\Delta\tau_x = 0.2$. For the 1st-order step scheme, numerical smearing error decreases linearly with grid size, as expected from Eq. (4) with n = 1. For the higher-

order schemes, the decrease in error with increasing grid resolution is nonlinear ($n > 1$ in Eq. (4)). The positive scheme appears to provide a sufficient balance between accuracy and efficiency, as it does not require relaxation techniques necessary for the higher-order schemes.

An illustration of ray effect error due to finite angular discretization is presented in Figure 5a, where heat fluxes $Q(x^*, y^* = 0.5, z^* = 1.0)$, generated varying total direction number M are plotted and compared to MC predictions [Boulet et al. 2007]. To ensure grid independency and limit numerical smearing error, the spatial grid is taken to be $\Delta x^* = 0.04$. Angular resolution has a profound impact when the medium is thin (τ = 1.0), as ray effect manifests as unrealistic bumps in the heat flux profiles. Increase in angular resolution mitigates ray effect error. For the thick medium (τ = 10.0), ray effect is minimal, due to the large increase in scattering events in a CV, reducing ray propagation errors. This is consistent with the findings of Chai et al. [2003] and Raithby [1999]. Comparing the results from Figures 3 and 5a, it appears that while ray effect is dominant for thinner media, numerical smearing is dominant for thicker media.

Figure 5b plots percentage error in heat flux at the center of the far wall due to ray effect versus discrete solid angle $\Delta\Omega^l$ (where $\Delta\Omega^l = 4\pi/M$) for various medium optical thicknesses. Spatial grid is taken to be $\Delta x^* = 0.04$ to minimize numerical smearing. For constant optical thickness, refining angular grid resolution reduces ray effect error. Ray effect error decreases with increasing optical thickness for all examined spatial grids, due to an increase in total scattering events and ray attenuation. Error due to ray effect is less than 2% for $\Delta\Omega^l \leq 0.0785$ ($M \geq 160$) for all optical properties, indicating that further refinement of angular resolution is unnecessary to generate accurate results. Comparing the results in Figures 3-5, it is noticed that reduction of $\Delta\tau$ can reduce both error types without corresponding or necessary change in M or μ^l. However, an increase in M mandates a necessary decrease in $\Delta\tau$, in order to ensure minimization of both error sources.

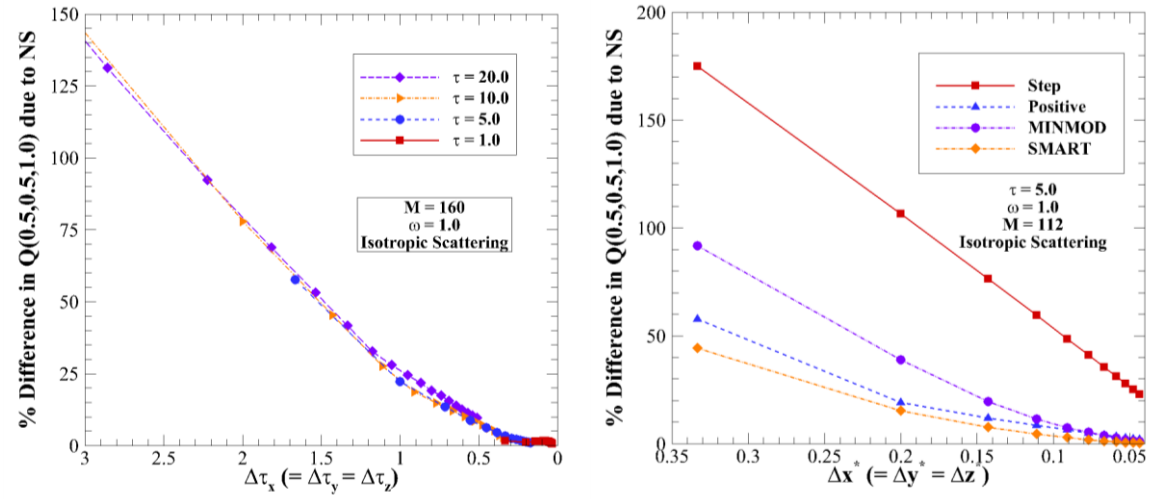

Figure 4: Effect of a) dimensionless grid size $\Delta\tau$ and b) spatial differencing scheme on numerical smearing

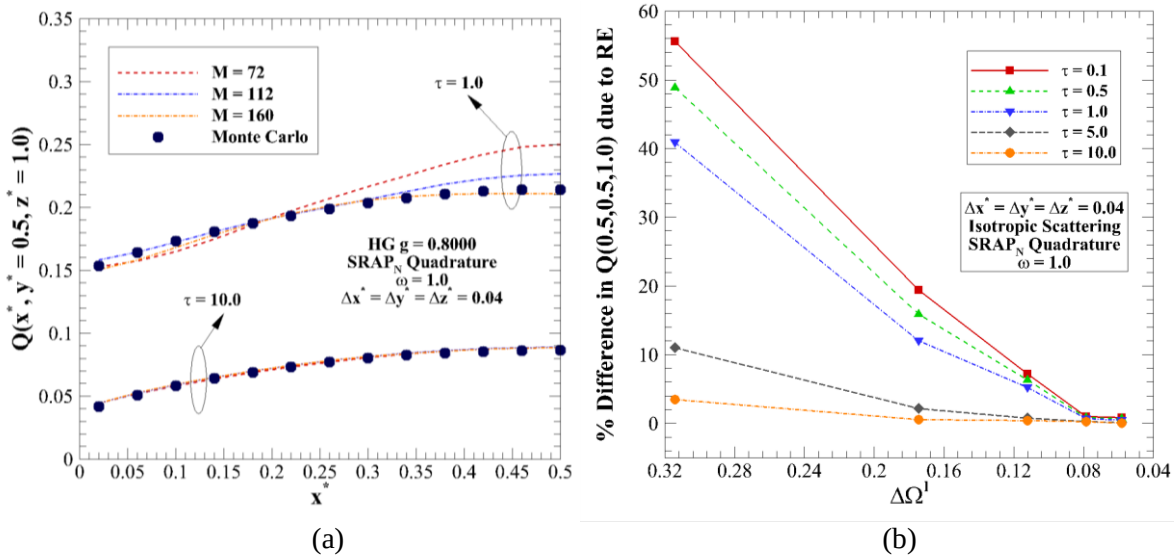

(a) (b)

Figure 5: Impact of discrete direction number and optical thickness on ray effect error.

CONCLUSION

In this study, the impacts of two prominent numerical errors, namely numerical smearing and ray effect, on DOM radiation transfer predictions are investigated and examined in detail. Proportionality expressions are derived for numerical smearing errors, and ray effect is further classified into local and propagation components. The analysis revealed, for the first time, the relationship between numerical smearing and the ratio $\Delta\tau_x/\mu^l$, indicating dependence on both angular and spatial discretization. It becomes critical to ensure that ratio is less than unity, to ensure minimal numerical smearing error. Ray effect error is shown to be comprised of local and propagation errors, the latter of which affects radiation intensity at all adjacent CVs via spatial interpolation. Ray propagation errors can be reduced via spatial grid refinement, while local error can be reduced via increasing $\Delta\tau$. Most importantly, reduction of $\Delta\tau$ is able to reduce both numerical smearing and propagation ray effect without a necessary change in direction number, although an increase in direction number mandates a necessary decrease in $\Delta\tau$ in order to minimize both error sources.

REFERENCES

Boulet, P., Collin, A., and Consalvi, J.L. [2007] On the finite volume method and the discrete ordinates method regarding radiative heat transfer in acute forward anisotropic scattering media, *J. Quant. Spectrosc. Radiat. Transfer*, Vol. 104, pp. 460-473.

Chai, J.C., Lee, H.S., and Patankar, S.V. [1993], Ray effect and false scattering in the discrete ordinates method, *Num. Heat Transfer B*, Vol. 24, pp. 373-389.

Coelho, P.J. [2002], The role of ray effects and false scattering on the accuracy of the standard and modified discrete ordinates method, *J. Quant. Spectrosc. Radiat. Transfer*, Vol. 73, pp. 231-238.

Howell, J.R., Siegel, R., and Menguc, M.P. [2011] Thermal Radiation Heat Transfer, CRC Press, Boca Raton, Fla.

Hunter, B. and Guo, Z. [2011], Comparison of discrete-ordinates method and finite volume method for steady-state and ultrafast radiative transfer analysis in cylindrical coordinates, *Num. Heat Transfer B*, Vol. 59, pp. 339-359.

Hunter, B. and Guo, Z. [2012], Conservation of asymmetry factor in phase function discretization for radiative transfer analysis in anisotropic scattering media, *Int. J. Heat Mass Transf.*, Vol. 55, pp. 1544-1552.

Hunter, B. and Guo, Z. [2013], Comparison of quadrature schemes in DOM for anisotropic scattering radiative transfer analysis, *Num. Heat Transfer B*, Vol. 63, pp. 485-507.

Menguc, M.P. and Viskanta, R. [1985], Radiative transfer in three-dimensional rectangular enclosures containing inhomogeneous, anisotropically scattering media, *J. Quant. Spectrosc. Radiat. Transfer*, Vol. 33, No. 6, pp. 533-549.

Modest, M.F. [2003]. *Radiative Heat Transfer,* Academic Press, New York.

Raithby, G.D. [1997], Evaluation of discretization errors in finite-volume radiant heat transfer predictions, *J. Thermophys. Heat Transfer,* Vol. 11, pp. 540-548.